Effects of Transverse Shearing on Cylindrical Bending, Vibration, and Buckling of Laminated Plates

Manuel Stein* and Dawn C. Jegley†
NASA Langley Research Center, Hampton, Virginia

The displacements for cylindrical bending and stretching of laminated and thick plates are expressed through the thickness by a few algebraic terms and a complete set of trigonometric terms. Only a few terms of this series are needed to get sufficiently accurate results for laminated and thick plates. Equations of equilibrium based on a sufficient number of terms of this series for displacements are determined using variational theorems from three-dimensional elasticity. Several examples are worked out. The displacements and stresses are obtained for simply supported isotropic and layered plate strips (beams with a rectangular cross section) and sinusoidal lateral load distribution. These results are compared to an exact elasticity solution. Results for several approximations are obtained for a simply supported and a clamped beam loaded at the center, and results are compared to experimental results. Results are also obtained for isotropic and layered beams for several approximations for the lowest natural frequency and buckling load.

Nomenclature

d	= applied displacement
E,E_z	= Young's modulus of elasticity in the length and thickness directions, respectively
G_{xz}	= transverse shear modulus
h	= beam thickness
L	= beam length
P	= applied load
P_0	= magnitude of applied sinusoidal load
u,w	= beam displacements
x,y,z	= coordinate directions
ϵ_x,ϵ_z	= direct strains
γ_{xz}	= transverse shear strain
σ_x,σ_z	= direct stresses
$\sigma_{x_{cr}}$	= stress at buckling
τ_{xz}	= transverse shear stress
ω	= frequency of vibration

Introduction

CLASSICAL plate cylindrical bending theory predicts deformations and longitudinal stresses that are comparable to the actual deformations and longitudinal stresses given by three-dimensional elasticity for thin beams and plates of homogenous materials. Conventional transverse shearing theory makes similar predictions for sandwich construction and for thicker beams and plates of homogenous materials. An average value of the transverse shear stress can be found from the deformations using the strain-displacement relation and conventional transverse shearing theory. However, reasonably accurate distributions of transverse shear stress and transverse normal stress can only be found for isotropic beams or plates from a special solution that uses beam results and elasticity theory. Simple, dependable approaches are needed for obtaining transverse stresses for structures made of a nonhomogeneous material such as laminated composites. Determining accurately the transverse shear stress and transverse normal stress, in addition to the displacements and longitudinal stress, can be important for beams or plates, even though the transverse stresses are small compared to the longitudinal stress. These transverse stresses are important when the structures are relatively weak in the transverse direction and when the response behavior is sensitive to the transverse stiffness. It is well known that the higher modes of vibration are sensitive to transverse effects associated with three-dimensional elasticity and, from sandwich theory, it is known that buckling is sensitive to transverse shearing stiffness.

The need for more accurate analyses for laminated beams and plates has led to a number of new theories that have appeared in the literature (e.g., Refs. 1–9). The theories that have appeared are all linear, use displacements expressed by the first few terms of a power series in the coordinate through the thickness, and may satisfy natural boundary conditions at the plate surface or may use transverse shear stiffness correction factors. Almost any theory may be altered to include nonlinear effects, and any additional terms used to express the displacements will improve the accuracy if an acceptable method of analysis is used. To get a tractable solution with nonlinear terms and to keep the unknowns to a minimum requires that careful choices be made. Also, estimates from three-dimensional elasticity of the transverse stresses when in-plane stresses and deformations have been given by elementary theory do not give the effect of the transverse stiffnesses on the in-plane stresses and deformations and do not give the transverse deformations. With regard to satisfaction of natural boundary conditions, if the potential energy method is used, continuity of displacements is satisfied, but it is not necessary to satisfy natural boundary conditions. If natural boundary conditions are satisfied by constraints on an approximate potential energy solution, it is inefficient because the full use of the assumed approximation is unnecessarily restricted by these constraints. If the complementary energy method is used, it is not necessary to satisfy continuity, but equilibrium of ex-

Presented as Paper 85-0774 at the AIAA/ASME/ASCE/AHS 26th Structures, Structural Dynamics and Materials Conference, Orlando, FL, April 15–17, 1985; received May 23, 1985; revision received April 17, 1986.

*Senior Aerospace Engineer, Structural Mechanics Branch, Structures and Dynamics Division. Associate Fellow AIAA.

†Aerospace Engineer, Structural Mechanics Branch, Structures and Dynamics Division. Member AIAA.

ternal force conditions, including natural boundary conditions, must be satisfied. Similarly, satisfying continuity in an approximate complementary energy solution is inefficient. It is on a physical basis, together with some results of trial calculations, that the present theory chooses to use trigonometric terms instead of additional terms in a power series in z to represent the through-the-thickness (z) behavior of plates beyond that given by conventional transverse shear theory. The present approach is a formal approach starting from three-dimensional nonlinear elasticity and is different from other methods available in the literature.

The present approach differs from other methods in that the displacements have trigonometric terms in addition to the first few terms of the power series for the displacements. The present approach makes use of both the potential and complementary energy methods; the surface conditions are satisfied by the complementary energy method, but surface conditions are not satisfied in the potential energy method since these constraints are not required for this method. No attempt is made to improve the accuracy of some terms by using an arbitrary shear correction factor. This approach was also used in Ref. 10 to develop a theory of two-dimensional plates and shells. In Ref. 10 and in the present paper, a trigonometric series is used to represent the unknowns in terms of the through-the-thickness coordinate. Potential energy and complementary energy methods are used so that few terms in the series can be used to get accurate displacements or stresses. Assumptions are used to simplify the nonlinear strains of three-dimensional elasticity, to choose the number of terms in the series, and to pick the appropriate stress-strain law. The series are specified so that the first term in the series will lead to conventional transverse shearing theory and, for small beam or plate thickness, conventional transverse shearing theory reduces to classical theory. Generally, one trigonometric term is retained for each displacement to assure sufficient accuracy. Results obtained from classical theory, from conventional transverse shearing theory, and from the present approach are compared with each other and with results from an elasticity solution or with results from experiment. Comparisons of results of various approaches are also presented for the lowest natural frequency and buckling load for both isotropic and layered materials.

Analysis

A theory accurate enough to determine transverse shear and normal stresses is developed from cylindrical bending of a plate. Geometrically nonlinear effects are included in the strains. Displacements are written in a general algebraic and trigonometric series in the through-the-thickness (z) direction. Strains and displacements are specialized to the approximation desired for the problems considered and equations, and then results are determined from either the potential energy method or the complementary energy method. Figure 1 indicates the coordinate system used, the axial and lateral displacements u and w, and length and thickness dimensions L and h.

For the present analysis, stresses and deformations are considered to be independent of y and the stress $\sigma_y = 0$. The strains (e.g., Ref. 11) based on the change in length of material lines in the coordinate directions and on the change in angle between them are

$$\epsilon_x = \sqrt{(1+u_{,x})^2 + w_{,x}^2} - 1$$

$$\epsilon_z = \sqrt{(1+w_{,z}^2) + u_{,z}^2} - 1$$

$$\gamma_{xz} = \sin^{-1}\left[\frac{(1+u_{,x})u_{,z} + (1+w_{,z})w_{,x}}{\{[(1+u_{,x})^2 + w_{,x}^2][u_{,z}^2 + (1+w_{,z})^2]\}^{1/2}}\right] \tag{1}$$

Retaining terms to second degree in u and w and their derivations gives the approximate strains

$$\epsilon_x = u_{,x} + \tfrac{1}{2} w_{,x}^2$$

$$\epsilon_z = w_{,z} + \tfrac{1}{2} u_{,z}^2$$

$$\gamma_{xz} = u_{,z} + w_{,x} - w_{,x}u_{,x} - w_{,z}u_{,z} \tag{2}$$

In general the displacement u can be represented by

$$u = u_0(x) + \frac{z}{h}u_a(x) + \left(\frac{z}{h}\right)^2 u_{2a}(x) + \sum_{n=1,3,5}^{\infty}\left(u_{ns}(x)\sin\frac{n\pi z}{h} + u_{nc}(x)\cos\frac{n\pi z}{h}\right) \tag{3}$$

and a similar series could represent the displacement w. The trigonometric terms included in the summation are a complete set, and they can represent any function in the interval $(-h/2<z<h/2)$. The three algebraic terms are added arbitrarily to the series so that boundary conditions in the z direction can be better represented when only a few trigonometric terms are used in an approximate analysis.

Potential Energy (Virtual Work)

The virtual work for a plate (beam of rectangular cross section) of unit width is

$$\delta\pi_P = \int_0^L \int_{-h/2}^{h/2} [\sigma_x\delta\epsilon_x + \sigma_z\delta\epsilon_z + \tau_{xz}\delta\gamma_{xz} - \mu\omega^2(w\delta w + u\delta u)]\,\mathrm{d}z\mathrm{d}x + \int_0^L \left[P_{h/2}\delta w\left(x,\frac{h}{2}\right) + P_{-h/2}\delta w\left(x,-\frac{h}{2}\right)\right]\mathrm{d}x \tag{4}$$

where the first three terms represent the work of internal forces, the $\mu\omega^2$ terms represent the work of the inertia forces, and the other terms represent the work of the surface pressures. The terms considered for the displacements are now limited to

$$u = u_0(x) + u_a(x)\frac{z}{h} + u_{1s}(x)\sin\frac{\pi z}{h}$$

$$w = w_0(x) + w_{1c}(x)\cos\frac{\pi z}{h} \tag{5}$$

In application of the equations developed here, u_0 appears only in the buckling terms. For reduction to classical (Kirchhoff) theory, identified as $\tau_{xz}=0$ or conventional transverse shearing (Timoshenko) theory, identified as $\tau_{xz}=\tau_{xz}(x)$, the u_{1s} and w_{1c} terms are neglected. The most accurate potential energy solution presented here, identified as $\tau_{xz}=\tau_{xz}(x,z)$, includes the first trigonometric terms as shown in Eq. (5). All terms used in the u displacement series except u_0 are antisymmetric in z, while all terms used in the

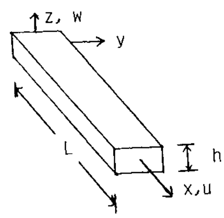

Fig. 1 Dimensions and coordinate system of beam.

w displacement series are symmetric. One way of obtaining equations equivalent to classical theory from conventional transverse shearing theory is by requiring that $u_a = -w_{0,x}$. Substituting Eq. (5) for the displacements in Eqs. (2) and retaining only the largest nonlinear term results in the strains

$$\epsilon_x = u_{0,x} + \frac{1}{2} w_{0,x}^2 + u_{a,x} \frac{z}{h} + u_{1s,x} \sin \frac{\pi z}{h}$$

$$\epsilon_z = -\frac{\pi}{h} w_{1c} \sin \frac{\pi z}{h}$$

$$\gamma_{xz} = \frac{u_a}{h} + w_{0,x} + \left(\frac{\pi}{h} u_{1s} + w_{1c,x}\right) \cos \frac{\pi z}{h}$$

When the variations of the various displacement coefficients are taken, integration by parts leads to the following differential equations

$$\int_{-h/2}^{h/2} (-\sigma_{x,x} - \mu\omega^2 u_0) dz = 0$$

$$\int_{-h/2}^{h/2} \left[-\sigma_{x,x} \frac{z}{h} + \frac{1}{h}\tau_{xz} - \mu\omega^2 \left(u_a \frac{z}{h} + u_{1s} \sin \frac{\pi z}{h}\right) \frac{z}{h}\right] dz = 0$$

$$\int_{-h/2}^{h/2} \left[-\sigma_{x,x} \sin \frac{\pi z}{h} + \frac{\pi}{h} \tau_{xz} \cos \frac{\pi z}{h} - \mu\omega^2 \times \left(u_a \frac{z}{h} + u_{1s} \sin \frac{\pi z}{h}\right) \sin \frac{\pi z}{h}\right] dz = 0$$

$$\int_{-h/2}^{h/2} [-(\sigma_x w_{0,x})_{,x} - \tau_{xz,x} - \mu\omega^2 w_0] dz + P_{h/2} + P_{-h/2} = 0$$

$$\int_{-h/2}^{h/2} \left(-\sigma_z \frac{\pi}{h} \sin \frac{\pi z}{h} - \tau_{xz,x} \cos \frac{\pi z}{h} - \mu\omega^2 w_{1c} \cos \frac{\pi z}{h}\right) dz = 0 \tag{6}$$

and the following variationally consistent boundary conditons at $x = 0, L$

$$\int_{-h/2}^{h/2} \sigma_x dz \delta u_0 = 0 \qquad \int_{-h/2}^{h/2} (\sigma_x w_{0,x} + \tau_{xz}) dz \delta w_0 = 0$$

$$\int_{-h/2}^{h/2} \sigma_x \frac{z}{h} dz \delta u_a = 0 \qquad \int_{-h/2}^{h/2} \tau_{xz} \cos \frac{\pi z}{h} dz \delta w_{1c} = 0$$

$$\int_{-h/2}^{h/2} \sigma_x \sin \frac{\pi z}{h} \delta u_{1s} = 0 \tag{7}$$

With Hooke's law taken in the simple form

$$\sigma_x = E\epsilon_x \qquad \sigma_z = E_z \epsilon_z \qquad \tau_{xz} = G_{xz}\gamma_{xz} \tag{8}$$

where the stiffnesses E, E_z, and G_{xz} may be functions of z, it is apparent that the stresses will involve the same displacement coefficient functions of x as the strains. Equations equivalent to classical theory can be obtained from conventional transverse shearing theory equations, as mentioned before, by requiring that $u_a = -w_{0,x}$ before using the variational method so that γ_{xz} is zero or by allowing the thickness-to-length ratio to approach zero or by requiring that G_{xz} approach infinity.

Complementary Energy (Virtual Complementary Energy)

The virtual complementary energy for a plate (beam of rectangular cross section) of unit width is

$$\delta\pi_c = \int_0^L \int_{-h/2}^{h/2} \{\epsilon_x \delta\sigma_x + \epsilon_z \delta\sigma_z + \gamma_{xz}\delta\tau_{xz} + \delta[\alpha(\sigma_{x,x} + \tau_{xz,z}) + \beta(\sigma_{z,z} + \tau_{xz,x})]\} dz dx + \int_{-h/2}^{h/2} w\delta\sigma_z |_{x=L/2} dz \tag{9}$$

where the first three terms represent the work of the internal forces. The next group of terms requires that equilibrium is satisfied through the use of the Lagrangian multipliers α and β. The last term represents the work of a centrally applied w displacement. The only terms considered for the displacements are

$$u = u_a(x) \frac{z}{h} + u_{1s}(x) \sin \frac{\pi z}{h}$$

$$w = w_0(x) + w_{2a}(x) \left(\frac{z}{h}\right)^2 + w_{1c}(x) \cos \frac{\pi z}{h} \tag{10}$$

The w_{2a} term is included here to provide additional accuracy in σ_z. By substituting Eqs. (10) for the displacements in Eqs. (2) and retaining only results from linear terms

$$\epsilon_x = u_{a,x} \frac{z}{h} + u_{1s,x} \sin \frac{\pi z}{h}$$

$$\epsilon_z = \frac{2}{h} w_{2a} \frac{z}{h} - w_{1c} \frac{\pi}{h} \sin \frac{\pi z}{h}$$

$$\gamma_{xz} = \frac{1}{h} u_a + w_{0,x} + w_{2a,x}\left(\frac{z}{h}\right)^2 + \left(\frac{\pi}{h} u_{1s} + w_{1c,x}\right) \cos \frac{\pi z}{h} \tag{11}$$

Again, with Hooke's law taken in the simple form (8),

$$\sigma_x = E\epsilon_x \qquad \sigma_z = E_z\epsilon_z \qquad \tau_{xz} = G_{xz}\gamma_{xz}$$

where E, E_z, and G_{xz} may be functions of z, the stresses are of the form

$$\sigma_x = \sigma_{x_a} u_{a,x} + \sigma_{x_1} u_{1s,x}$$

$$\sigma_z = \sigma_{z_a} w_{2a} + \sigma_{z_1} w_{1c}$$

$$\tau_{xz} = \tau_{xz_0}\left(\frac{u_a}{h} + w_{0,x}\right) + \tau_{xz_{2a}} w_{2a,x} + \tau_{xz_1}\left(\frac{\pi}{h} u_{1s} + w_{1c,x}\right) \tag{12}$$

where the stress coefficients σ_{xa}, σ_{x1},... are functions of z only. The multipliers α and β can be represented in a form similar to u and w as

$$\alpha = \alpha_a(x) \frac{z}{h} + \alpha_{1s}(x) \sin \frac{\pi z}{h}$$

$$\beta = \beta_0(x) + \beta_{2a}(x)\left(\frac{z}{h}\right)^2 + \beta_{1c}(x) \cos \frac{\pi z}{h} \tag{13}$$

Variation with respect to the unknown coefficients (which are functions of x) gives the following differential equations in x:

$$\int_{-h/2}^{h/2}\left(-\sigma_{x_a}\epsilon_{x,x}+\frac{1}{h}\tau_{xz_0}\gamma_{xz}+\sigma_{x_a}\alpha_{,xx}+\frac{1}{h}\tau_{xz_{0,z}}\alpha-\frac{1}{h}\tau_{zx_0}\beta_{,x}\right)\mathrm{d}z=0$$

$$\int_{-h/2}^{h/2}\left(-\sigma_{x_1}\epsilon_{x,x}+\frac{\pi}{h}\tau_{xz_1}\gamma_{xz}+\sigma_{x_1}\alpha_{,xx}+\frac{\pi}{h}\tau_{xz_{1,z}}\alpha-\frac{\pi}{h}\tau_{xz_1}\beta_{,x}\right)\mathrm{d}z=0$$

$$\int_{-h/2}^{h/2}(-\tau_{xz_0}\gamma_{xz,x}-\tau_{xz_0}\beta_{,x})\mathrm{d}z=0$$

$$\int_{-h/2}^{h/2}(\sigma_{z_{2a}}\epsilon_z-\tau_{xz_{2a}}\gamma_{xz,x}-\tau_{xz_{2a,z}}\alpha_{,x}+\sigma_{z_{2a,z}}\beta+\tau_{xz_{2a}}\beta_{,xx})\mathrm{d}z=0$$

$$\int_{-h/2}^{h/2}(\sigma_{z_1}\epsilon_z-\tau_{xz_1}\gamma_{xz,x}-\tau_{xz_{1,z}}\alpha_{,x}+\sigma_{z_{1,z}}\beta+\tau_{xz_1}\beta_{,xx})\mathrm{d}z=0$$

$$\int_{-h/2}^{h/2}(\sigma_{x,x}+\tau_{xz,z})\frac{z}{h}\,\mathrm{d}z=0$$

$$\int_{-h/2}^{h/2}(\sigma_{x,x}+\tau_{xz,z})\sin\frac{\pi z}{h}\,\mathrm{d}z=0$$

$$\int_{-h/2}^{h/2}(\sigma_{z,z}+\tau_{xz,x})\mathrm{d}z=0$$

$$\int_{-h/2}^{h/2}(\sigma_{z,z}+\tau_{xz,x})\left(\frac{z}{h}\right)^2\mathrm{d}z=0$$

$$\int_{-h/2}^{h/2}(\sigma_{z,z}+\tau_{xz,x})\cos\frac{\pi z}{h}\,\mathrm{d}z=0 \tag{14}$$

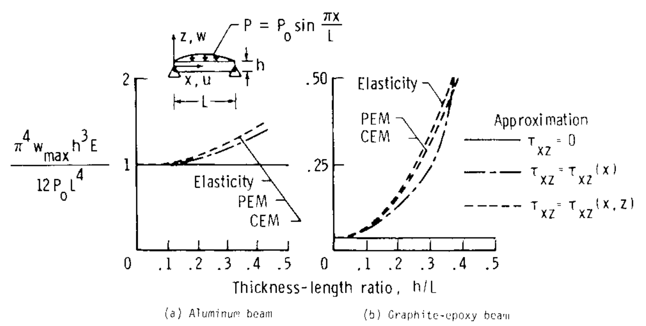

Fig. 2 Comparison of center deflection w_{max} obtained by potential (PEM) and complementary (CEM) energy methods with the exact solution from elasticity.

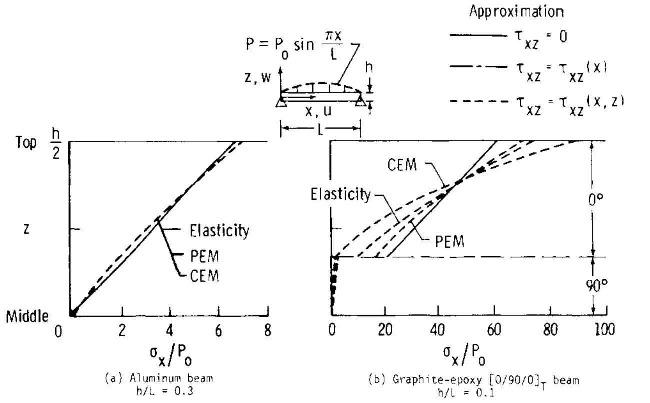

Fig. 3 Comparison of axial stress obtained by the potential (PEM) and complementary (CEM) energy methods with exact results obtained from elasticity.

and the following variationally consistent boundary conditions:

at $x=0,\ L/2$;

$$\int_{-h/2}^{h/2}\left(\sigma_{x_a}(\epsilon_x-\alpha_{,x})+\frac{1}{h}\tau_{xz_0}\beta\right)\mathrm{d}z\delta u_a=0$$

$$\int_{-h/2}^{h/2}\left(\sigma_{x_1}(\epsilon_x-\alpha_{,x})+\frac{\pi}{h}\tau_{xz_1}\beta\right)\mathrm{d}z\delta u_{1s}=0$$

$$\int_{-h/2}^{h/2}\tau_{xz_0}(\gamma_{xz}+\beta)\mathrm{d}z\delta w_0=0$$

at $x=L/2$;

$$\int_{-h/2}^{h/2}[\tau_{xz_{2a}}(\gamma_{xz}-\beta_{,x})+\tau_{xz_{2a,z}}\alpha-\sigma_{z_{2a}}w]\mathrm{d}z\delta w_{2a}=0$$

$$\int_{-h/2}^{h/2}[\tau_{xz_1}(\gamma_{xz}-\beta_{,x})+\tau_{xz_{1,z}}\alpha-\sigma_{z_1}w]\mathrm{d}z\delta w_{1c}=0$$

at $x=0$;

$$\int_{-h/2}^{h/2}[\tau_{xz_1}(\gamma_{xz}-\beta_{,x})+\tau_{xz_{1,z}}\alpha]\mathrm{d}z\delta w_{1c}=0$$

$$\int_{-h/2}^{h/2}[\tau_{xz_{2a}}(\gamma_{xz}-\beta_{,x})+\tau_{xz_{2a,z}}\alpha]\mathrm{d}z\delta w_{2a}=0$$

at $x=0,\ L/2$;

$$\int_{-h/2}^{h/2}\sigma_{x_a}\alpha\mathrm{d}z\delta u_{a,x}=0 \qquad \int_{-h/2}^{h/2}\tau_{xz_{2a}}\beta\mathrm{d}z\delta w_{2a,x}=0$$

$$\int_{-h/2}^{h/2}\sigma_{x_1}\alpha\mathrm{d}z\delta u_{1s,x}=0 \qquad \int_{-h/2}^{h/2}\tau_{xz_1}\beta\mathrm{d}z\delta w_{1c,x}=0 \tag{15}$$

Equations (14) and boundary conditions [Eqs. (15)] are solved numerically to obtain results from the complementary energy method, which are discussed in the following section.

Applications

The equations that have been derived are applied to five examples of loading and boundary conditions: a sinusoidal lateral loading on a simply supported beam, a central displacement applied to a clamped and to a simply supported beam, a simply supported beam vibrating at its lowest natural frequency, and the critical buckling load of a simply supported beam. The potential energy method is applied to all examples considered. The complementary energy method is applied to only the first three examples. Each loading is applied to an isotropic (aluminum) one-layer beam and a laminated three-layer graphite-epoxy beam of $[0°/90°/0°]_T$ layup in which all layers have the same thickness.

The material properties for the laminated beam involve a ratio of 25:1 for the stiffnesses of the 0° ply to the 90° ply and, a ratio of 2.5:1 for the through-the-thickness shear modulus of a 0° ply to the 90° ply. A constant through-the-thickness stiffness is used. This stiffness (E_z) is equal to the extensional stiffness of the epoxy alone. Solutions are obtained using a classical approach in which the transverse shear stress is taken to be zero, an approach in which the transverse shear stress is taken to be dependent on the length coordinate only (constant through the thickness), and by taking the transverse shear stress to be dependent on both the length and depth coordinates.

Beam with Sinusoidal Lateral Load

The first example considered is a sinusoidal lateral pressure loading on a simply supported beam. Approximate results are obtained using both the potential and complementary energy methods, and an exact solution is obtained by solving the three-dimensional differential equations of elasticity. Results are presented for the maximum displacement of the beam in the z direction as a function of its thickness-to-length ratio h/L in Fig. 2. The classical approach in which the shear stress is taken to be zero ($\tau_{xz}=0$ on the figure) gives the w_{max} parameter a constant value for an isotropic beam $\pi^4 w_{max} h^3 E/(12 P_0 L^4)=1$. For the laminated beam the stiffness changes through the thickness, and this parameter is constant but not equal to one. To calculate this parameter, E is the stiffness in the x direction in the middle (90°) layer. Allowing the shear stress to depend only on the length coordinate [$\tau_{xz}=\tau_{xz}(x)$ on the figure] improves the accuracy of the solution. Notice that the maximum deflection increases more for the laminated beam than for the aluminum beam as h/L increases. More of an improvement in accuracy is made when the shear stress is taken to vary in both the x and z directions [$\tau_{xz}=\tau_{xz}(x,z)$ on the figure], as shown by the solutions based on the present theory using the potential and complementary energy methods.

The normal and transverse stresses thrugh the depth for the aluminum beam, which has an h/L of 0.3, and for the graphite-epoxy beam, which has an h/L of 0.1, are shown in Figs. 3-5. Both potential and complementary energy methods give accurate results for all three stresses in the aluminum beam. In Fig. 3b the axial stress is discontinuous at the layer interfaces due to a change in stiffness which is shown by the elasticity solution. The potential energy method gives a discontinuity and gives better results for the axial stresses than the complementary energy method. In Fig. 4b the transverse normal stress is not discontinuous through the depth when calculated by potential energy because the stiffness in the z direction does not change. Agreement between the various methods is similar to that obtained for the aluminum beam. In Fig. 5b the transverse shear stress is continuous at the layer interfaces given by elasticity and the complementary energy method. However, the potential energy method is not required to satisfy equilibrium through the depth (using various approximations), and the potential energy method results are not continuous. This discontinuity can be eliminated by using many more terms in the assumed displacement series. The complementary energy method gives accurate transverse normal and transverse shear stresses (no discontinuities) but is not as good as the potential energy method in predicting the axial stress in the laminated beam.

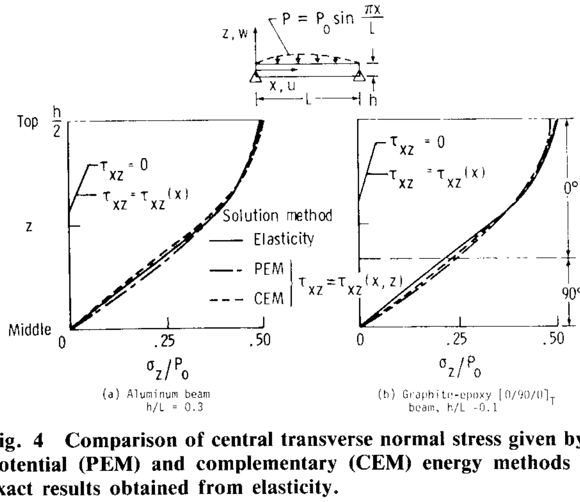

Fig. 4 Comparison of central transverse normal stress given by the potential (PEM) and complementary (CEM) energy methods with exact results obtained from elasticity.

Beam with Applied Central Displacement

Clamped Beam

The second example considered is a clamped beam with an applied central displacement. Results are presented for the three-layer $[0°/90°/0°]_T$ graphite-epoxy beam with a thickness-to-length ratio of 0.1. The distribution of the normal stresses, axial and transverse normal, and the transverse shear stress through the thickness of the beam are shown in Figs. 6 and 7, respectively. Here, both the potential and complementary energy methods give accurate results for the axial stress and differ markedly in the outer layers from the solution in which the shear stress is taken to be constant through the thickness. The complementary energy method is better at predicting the transverse normal stress since it accurately gives zero normal stress at the surface, while potential energy gives a maximum value at the surface. The transverse shear stress distribution shows the same discontinuity at the layer interfaces that occurs in the sinusoidal leading case for the potential energy method. This problem is resolved by using the complementary energy method.

Simply Supported Beams; Comparison with Experiment

An experiment described in Ref. 12 provides data on the distribution of the transverse shear strain of a simply supported laminated beam with an applied displacement or concentrated load. The material properties of the test specimen must be known to make a comparison between the experimental results and the prediction of the present analysis. The specimen used in this experiment was made of unidirectional T300/5208 graphite-epoxy material. The stiffnesses of this material are $E=19.0\times10^6$ psi in the x direction and

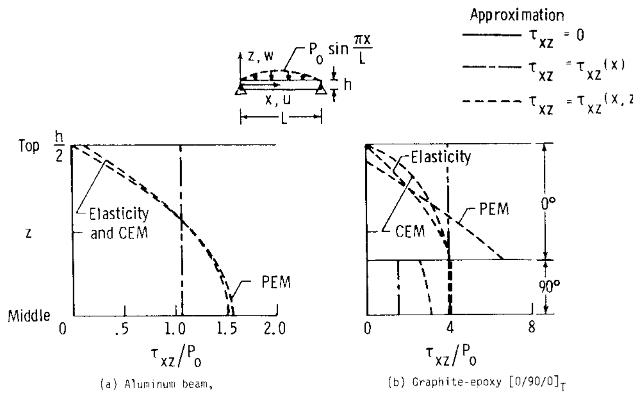

Fig. 5 Comparison of central transverse shear stress obtained by potential (PEM) and complementary (CEM) energy methods with exact results obtained from elasticity.

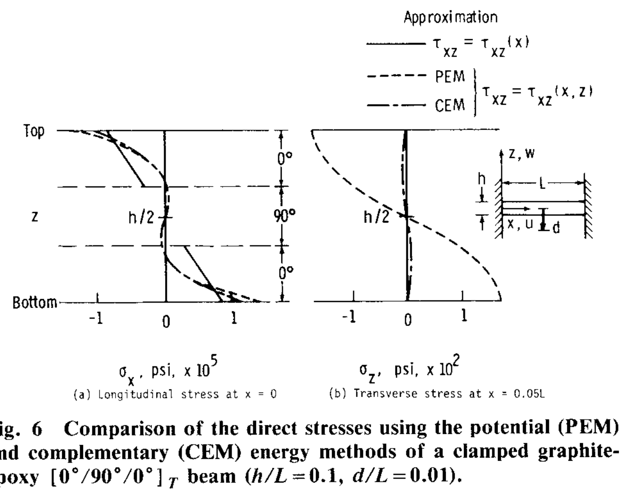

Fig. 6 Comparison of the direct stresses using the potential (PEM) and complementary (CEM) energy methods of a clamped graphite-epoxy $[0°/90°/0°]_T$ beam ($h/L=0.1$, $d/L=0.01$).

$E_z = 1.89 \times 10^6$ psi in the z direction. The thickness of the specimen used was $h = 0.283$ in. Since the specimen is unidirectional, all layers have the same through-the-thickness shear modulus, so the potential energy method predicts a transverse shear stress with no discontinuities. The value of the through-the-thickness shear modulus is not well established for laminated beams and the through-the thickness shear modulus used determines how well the analytical methods agree with the experimental results. The value for the shear modulus used was determined by a parametric study of a simply supported beam with an applied deflection at midlength (third example) using values of through-the-thickness shear modulus ranging from 0.2×10^6 psi to 0.9×10^6 psi. The maximum shear strain as a function of the shear modulus is shown in Fig. 8. The experimental maximum shear strain agrees with the predicted maximum shear strain when the through-the-thickness shear modulus is about 0.5×10^6 psi. A comparison of the shear strain from experiment and from analytical methods when a shear modulus of 0.5×10^6 psi is used is shown in Fig. 9. The correlation between experiment and the present analysis may prove to be a useful way of finding the through-the-thickness shear modulus.

Natural Vibration of a Beam

The fourth example considered is a simply supported beam vibrating at its lowest natural frequency. The lowest natural frequency for aluminum and three-layer graphite-epoxy beams are shown as a function of the thickness-to-length ratio in Fig. 10. Results are shown for solutions in which the shear stress τ_{xz} is equal to zero, in which it is taken to be dependent on the length coordinate only, $\tau_{xz} = \tau_{xz}(x)$, and in which it is dependent on both the length and depth coordinates, $\tau_{xz} = \tau_{xz}(x,z)$, using the potential energy method. For very thin beams, all three approximations give the same result for the lowest natural frequency but, for the thicker beam, the approximate methods are less accurate since more transverse shearing is taking place. For an aluminum beam with a thickness-to-length ratio of 0.3, allowing the shear stress to be dependent on the length coordinate improves the solution by only 12% over the solution in which the shear stress is taken to be zero. The solution in which the shear stress is a function of the length and depth coordinates improves the predicted frequency by 13% over the $\tau_{xz} = 0$ solution. However, for the graphite-epoxy beam with a thickness-to-length ratio of 0.1, allowing the shear stress to depend on the length coordinate improves the solution by 24%, while allowing it to depend on the length and depth coordinates improves the solution by 32%. The nodes in the natural modes for higher natural frequencies in effect divide the beam up into shorter thicker beams so that, for accurate higher frequencies, thick beam theory is required and is more important than for lower frequencies.

Buckling of a Beam

The last loading condition considered is a simply supported beam with an applied compressive load. The critical stress for the aluminum and graphite-epoxy beams is shown in Fig. 11 as a function of the thickness-to-length ratio. Results are based on using the potential energy method. For the aluminum case, where little transverse shearing occurs, all approximations give similar results up to a thickness-to-length ratio of 0.15. For the laminated beam the different approximations give similar results up to a thickness-to-length ratio of 0.05. For example, in an aluminum beam with thickness-to-length ratio of 0.1, the difference between the buckling-load results for the approximations in which the shear stress is zero and nonzero is only 3%. However, in the graphite-epoxy beam with the same h/L value, allowing the shear stress to vary along the length improves the results for the buckling load by 58% over the results for the approximation in which the shear stress is taken to be zero, and allowing the shear stress to vary in both directions improves the buckling load by 73% over the $\tau_{xz} = 0$ solution.

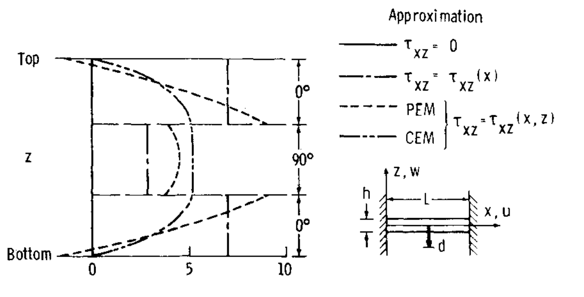

Fig. 7 Comparisons of the transverse shear stress using the potential (PEM) and complementary energy methods for a clamped graphite-epoxy beam $[0°/90°/0°]_T$ ($h/L = 0.1$, $d/L = 0.01$).

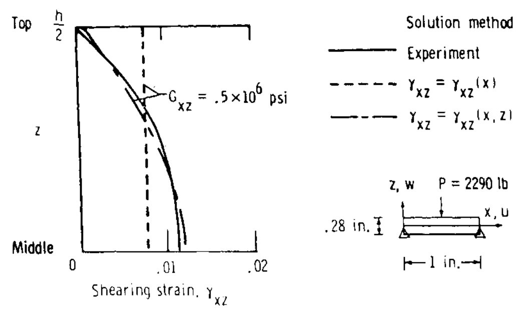

Fig. 9 Comparison of transverse shearing strain obtained by theory and experiment at $x = 0.25$ in. in a unidirectional T300/5208 graphite-epoxy beam.

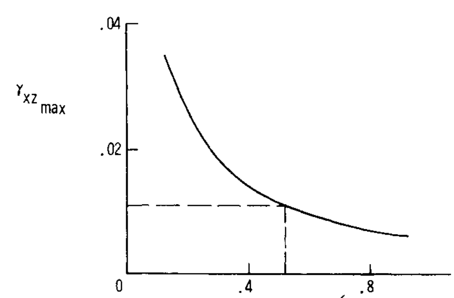

Fig. 8 Determination of a value of G_{xz} that correlates with experiment in a unidirectional T300/5208 graphite-epoxy beam.

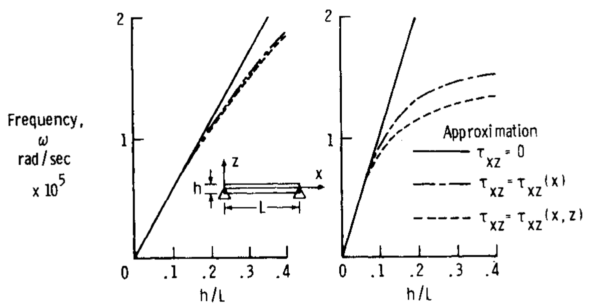

Fig. 10 Comparison of lowest natural frequency obtained by several approximations using the potential energy method.

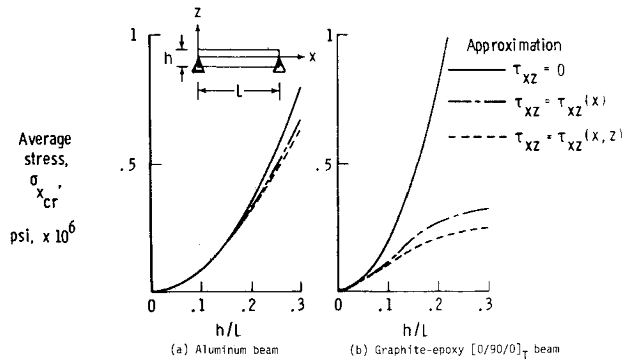

Fig. 11 Comparison of average stress at buckling obtained by several approximations using the potential energy method.

Concluding Remarks

A new theory for the analysis of beams of rectangular cross section is developed which incorporates trigonometric series in the assumed displacements and stresses. The present theory uses both the potential and complementary energy methods to find displacements and stresses. By including the first trigonometric term in each series, the accuracy of the stresses for a laminated composite beam or for a thick isotropic beam is significantly improved. For isotropic or unidirectional composite beams, the present theory accurately predicts displacements and stresses when either the potential or complementary energy method is used. For other laminated beams the present theory accurately predicts the displacements and axial stress by using the potential energy method and predicts the transverse normal and transverse shear stresses accurately by using the complementary energy method.

Often it is difficult to determine some of the transverse material properties in a structural component. With accurate theory and good experimental results, some relatively simple problems permit determination of these material properties. The through-the-thickness shear modulus is not easily found for laminated beams; application of the present theory illustrates a way of determining this material property.

Both the buckling load and the natural frequencies of a beam are significantly affected by transverse-shearing deformations especially in graphite-epoxy beams. The present theory indicates that by including trigonometric terms in the solutions, more accurate buckling loads and natural frequencies can be found.

References

[1] Whitney, J. M. and Pagano, N. J., "Shear Deformation in Heterogeneous Anisotropic Plates," *Journal of Applied Mechanics*, Vol. 37, No. 4, Dec. 1970, pp. 1031–1036.

[2] Chou, P. C. and Carleone, J., "Transverse Shear in Laminated Plate Theories," *AIAA Journal*, Vol. 11, Sept. 1973, pp. 1333–1336.

[3] Lo, K. H., Cristensen, R. M., and Wu, E. M., "A Higher-Order Theory of Plate Deformation, Part 2: Laminated Plates," *Journal of Applied Mechanics*, Vol. 44, No. 5, Dec. 1977, pp. 669–676.

[4] Levinson, M., "An Accurate, Simple Theory of the Statics and Dynamics of Elastic Plates," *Mechanics Research Communications*, Vol. 7, No. 6, 1980, pp. 343–350.

[5] Swift, G. W. and Heller, R. A., "Layered Beam Analysis," *Jounral of Engineering Mechanics*, Vol. 100, 1974, pp. 267–282.

[6] Reissner, E., "A Twelfth Order Theory of Transverse Bending of Transversely Isotropic Plates," *Zeitschrift für Angewandte Mathematik und Mechanik*, Vol. 63, 1983, pp. 285–289.

[7] Valisetty, R. R. and Rehfield, L. W., "A Theory for Stress Analysis of Composite Laminates," AIAA Paper 83-0833, May 1983.

[8] Reddy, J. N., "A Simple Higher-Order Theory for Laminated Composite Plates," *Journal of Applied Mechanics*, Vol. 51, Dec. 1984, pp. 745–752.

[9] Bhimaraddi, A. and Stephens, L. K., "A Higher Order Theory for Free Vibrations of Orthotropic, Homogeneous and Laminated Rectangular Plates," *Journal of Applied Mechanics*, Vol. 51, March 1984, pp. 195–198.

[10] Stein, M., "Nonlinear Theory for Plates and Shells Including the Effects of Transverse Shearing," *AIAA Journal*, Vol. 24, Sept. 1986, pp. 1537–1544.

[11] Novozhilov, V. V., *Foundations of the Nonlinear Theory of Elasticity*, Graylock Press, Rochester, NY, 1953.

[12] Post, D., Czarnek, R., Joh, D., and Wood, J., "Deformation Measurements of Composite Multi-span Beam Shear Specimens by Moire Interferometry," NASA CR-3844, Nov. 1984.